*Key Engineering Materials*
*ISSN: 1662-9795, Vol. 926, pp 1030-1038*
*doi:10.4028/p-ic4qyv*

*Submitted: 2021-12-08*
*Revised: 2022-01-24*
*Accepted: 2022-02-04*
*Online: 2022-07-22*

# Investigation of the Plane Strain Behaviour of a Laser-Heat Treated Aluminium Alloy

Antonio Piccininni[1,a*], Attilio Lattanzi[2,b], Marco Rossi[2,c] and Gianfranco Palumbo[1,d]

[1]Department of Mechanical Engineering, Mathematics & Management Engineering, Division of Production Technologies, Polytecnic University of Bari, via Orabona 4, 70125 Bari, Italy

[2]Department of Industrial Engineering and Mathematical Sciences, Università Politecnica delle Marche, via Brecce Bianche 12, 60131 Ancona, Italy

[a]antonio.piccininni@poliba.it, [b]a.lattanzi@staff.univpm.it, [c]m.rossi@staff.univpm.it, [d]gianfranco.palumbo@poliba.it

**Keywords:** laser heat treatment; aluminium alloy; Finite Element model; plane strain behaviour.

**Abstract.** The necessity of complex-shaped components characterized by superior mechanical properties and limited weight is moving the attention to the Aluminium (Al) alloys. Deep Drawing Steel grades possess superior stamping characteristics and formability with respect to Al alloys. But the need of light-weighting pushes towards the adoption of materials with optimal strenght-to-weight ratio, like Al alloys. Todays Al alloys are certainly used in the transport sector but their formability (at room temperature) is poorer than Deep Drawing Steel grades, which still hinders their massive implementation in the forming processes and drives the research toward innovative manufacturing solutions. One of the most promising approach to overcome such a limitation and, thus, manufacture complex component using cold forming processes, is the adoption of local heat treatments to obtain a suitable distribution of material properties able to enhance the formability at room temperature.

The design of cold forming using locally modified blanks needs: (i) an extensive investigation of the material behaviour at room temperature after the local heating and (ii) the adoption of a Finite Element approach. As for the former aspect, the authors proposed a fast and comprehensive methodology to investigate the hardening behaviour of an Al alloy (AA5754-H32) locally annealed by laser heat treatment. Using a similar approach, the hardening model was then enriched by considering the normal anisotropy, evaluating the correlation between the Lankford parameter and the material condition reached at the end of the local treatment. To improve the knowledge on the plastic response of the material, the present work focusses on the characterization of the plane strain behavior of the AA5754, initially in wrought condition (H32) and subsequently modified by laser heating. In particular, the study proposes a new quasi-homogeneous specimen which combines the local heating profile with an optimized geometry to produce a prevailing plane strain condition in the heat-treated zone. In such a way, data about the material response in the plane strain condition could be obtained for a large range of material conditions determined by the preliminary heat treatment.

## Introduction

Aluminium (Al) and its alloys are a well-established class of metallic materials, within the big group of the light alloys, able to combine excellent material properties with a limited density (about one third of the steel one). For such reasons, Al alloys have been progressively referred as ideal candidate to achieve a sensible reduction of the vehicle masses, thus matching the continuously stringent limits in terms of harmful emissions [1]. Beside this, it should be underlined that, especially for railway applications, Al alloys are ranked as the best candidate since they do not produce smoke in case of fire [2].

Nevertheless, it is equally well-known that Al alloys are mostly limited by their poor formability at room temperature, which reflects in a lower geometrical complexity achievable at the end of the forming operation that, in turns, means to produce smaller and less complex sub-parts to be joined in a subsequent process steps (by riveting, welding or similar joining solutions).

The importance of reducing the masses of transportation vehicles has then pushed, over the last decades, the scientific research to find effective solutions to overcome the limitation of the poor formability: from one side, the increase of the working temperature has a direct effect on the material formability. In such a way, the forming operations carried out in warm conditions have shown promising results in achieving a superior complexity of the components, from smaller part to large-scale components for transportation [3,4]. At the same time, more innovative solutions have been investigated: the local modification of the material properties, prior to the stamping operations, has demonstrated its potentialities in enhancing the Al alloys formability at room temperature [5]. It has been demonstrated that, if the outer region of a 6xxx circular specimen is brought to the fully solutioned state – by means of short-term laser heating – and subsequently deep-drawn at room temperature, its formability can be improved up to 20% [6].

The process design, especially in the latter case, needs a systematic approach based on the numerical simulation that can properly assist in the tuning of the several process parameters, from those related to the local heating to those related to the stamping operations. The construction of an accurate numerical model passes through the definition of a proper material modelling: the most challenging aspect is to formulate a constitutive equation able to catch the heterogeneity of the material properties once it has been locally modified by the action of a short-term treatment. To achieve such an ambitious goal, it is equally important to rely on a robust characterization route able to provide the necessary data to calibrate the constants from the constitutive equations to be implemented within the numerical model.

Due to the strong heterogeneity of the material's properties full-field distribution once it has been locally modified, specific measurement techniques and advanced calibration methods are needed to collect the necessary data during the material characterization. For instance, in [7] the Digital Image Correlation (DIC) [8] is used to investigate the hardening behaviour of LHT specimens. In particular, the local variation of constitutive properties is studied by developing a spatial Fourier Expansions framework of the hardening law parameters, which are inversely calibrated with the Virtual Fields Method (VFM) [9]. One of the main advantages of coupling full-field measurements with inverse methods is the capability to perform the identification even by using non-homogeneous tests enriching the amount of material information provided from a single test. To this purpose, a wide class of identification strategies has been introduced to calibrate even complex material models [10]. Focusing on metal plasticity problems, for instance, in [14] an inverse method based on Finite Element simulations – also known as Finite Element Model Updating (FEMU) – is used to calibrate the Hill48 anisotropic plasticity model employing data from uniaxial and biaxial tensile tests. Energy approaches based on the Principle of Virtual Work as the VFM were employed for the identification the constitutive parameters of isotropic hardening models [12,13] allowing to include data from the post-necking regime, to characterize complex anisotropic plasticity models such as the Yld2000-2d [17,18] and, recently, to characterize the thermomechanical behaviour of a DP980 steel [16].

The present work can be regarded as a follow-up of the methodology already developed by the authors [17] and aimed to collect data regarding the mechanical behavior of a strain-hardenable Al alloy (AA5754), initially in the wrought conditions and locally annealed by means of a laser heating. The methodology has been then applied to evaluate the evolution of the anisotropy of the material as a function of the level of annealing reached at the end of the local heating [18]. In order to widen the knowledge of the material behaviour, the attention was moved on the investigation of stress states close to the plane strain condition. The objective is to investigate the influence of the annealing levels in stress states different from the uniaxial one using inverse methods. More in detail, different local heating strategies were numerically investigated on a conventional notched specimen aiming at: (i) locally bringing the material in the fully annealed condition and (ii) obtaining a gradient of properties within the notched region to gather the necessary data using only one test.

## Material and Methodology

**Material.** The alloy under investigation belongs to the group of the strain-hardenable Al alloys (AA5754); chemical composition is reported in Table 1.

**Table 1** Chemical composition of the investigated alloy

| | Al [%] | Cr [%] | Cu [%] | Fe [%] | Mg [%] | Mn [%] | Si [%] | Ti [%] | Zn [%] |
|---|---|---|---|---|---|---|---|---|---|
| AA5754-H32 | Bal. | 0.024 | 0.057 | 0.377 | 3.057 | 0.187 | 0.259 | 0.017 | 0.025 |

**Annealing investigation.** In the present section, the methodology to numerically predict the level of annealing is briefly described according to [17]. Local annealing treatments were physically simulated with the Gleeble system (model 3180) on dog-bone specimens (AA5754-H32). A specific temperature profile was applied, based on a preliminary heating step (heating rate at 900°C/s), holding at the test temperature (10 s) and rapid cooling down to room temperature. Thanks to the parabolic distribution of temperature during the test (the ends of the specimens are clamped by cooled jaws), temperature evolutions with time could be extracted from different locations along the longitudinal direction. The subsequent hardness measurements, carried out at room temperature, could be then univocally correlated with the relative temperature evolutions.

From the hardness measurements, a new variable *Ann* (see Equation 1) was defined to describe the level of annealing reached in a certain point according to its corresponding temperature evolution (the quantities $HV_{ar}$, $HV_{meas}$ and $HV_{min}$ refer to the hardness of the material in the as-received conditions, measured one and in the fully annealed state, respectively).

$$Ann = \frac{HV_{ar} - HV_{meas}}{HV_{ar} - HV_{min}}. \tag{1}$$

It was also demonstrated that the variable *Ann* could be analytically described by a logistic function describing its dependency with the peak temperature ($T_{peak}$), as expressed by Equation 2 [17].

$$Ann = \frac{1}{1+\exp\left[-\lambda\cdot\left(T^{*}-T_{peak}\right)\right]}. \tag{2}$$

In this shape, the level of annealing is related to the peak temperature with no explicit expression of the effect on the constitutive properties of the aluminum alloy. Following the hybrid numerical-experimental procedure reported in [4, 5], the different hardening behaviour associated to each level of annealing can be also expressed through a general function of the peak temperature ($T_{peak}$):

$$\sigma\left(\varepsilon_p, T_{peak}\right) = \sigma_{ann}\left(\varepsilon_p\right) + \frac{\sigma_{ar}\left(\varepsilon_p\right) - \sigma_{ann}\left(\varepsilon_p\right)}{1+\exp\left\{-\left[\beta\tanh\left(\frac{\varepsilon_p}{\varepsilon_0}\right)+c_\beta\right]\left(T^{*}-T_{peak}\right)\right\}}, \tag{3}$$

where $\varepsilon_p$ is the plastic strain, the $\sigma_{ar}\left(\varepsilon_p\right)$ and $\sigma_{ann}\left(\varepsilon_p\right)$ indicates the flow curves of the material respectively in the *as-received* and *fully-annealed* conditions, and $\beta$, $\varepsilon_0$, $T^{*}$ and $c_\beta$ are the material coefficients of the logistic formulation. Basically, the idea is to modify the hardening response according to the level of annealing experienced by the material point.

**Two-stages numerical analysis.** The present work is focused on the investigation of the plane strain condition of a notched specimen, whose geometry was taken from literature [19], locally brought to the fully annealed condition by means of a laser heating. Figure 1 schematically depicts the adopted methodology: the local annealing treatment and the associated distribution of mechanical properties are simulated through a two-stages procedure based on Finite Element analyses. First, the laser heat treatment is numerically reproduced on a 3D transient thermal model by using the commercial code Abaqus/Standard®, and the temperature distribution imposed by the heating cycle is employed to predict the local level of annealing.

Then, the level of annealing achieved at each location on the specimen surface is converted to the corresponding material response in a 2D structural implicit analysis. This second step allow us to

have an insight of the overall deformation behaviour of the specimen, towards the evaluation of the strain (and stress) states generated during the test.

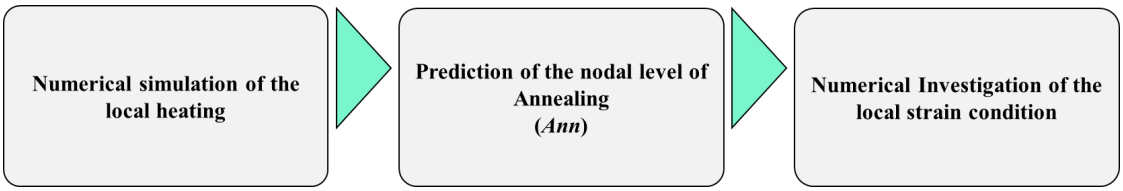


**Figure 1** Schematic description of the adopted methodology

Laser heating (10 mm square spot) was simulated according to three different strategies, described in Figure 2 (detailing the specimen's portion close to the notched area): (i) the *LT* strategy (acronym of *Linear Track*) based on a single linear track along the *y* axis direction; (ii) the *SPc* (acronym of *Spot_centered)* considering the laser spot located at the geometrical center of the notched specimen; (iii) the SPs (acronym of *Spot_shifted)* positioning the laser spot 3.75 mm (one quarter of the notch extension) far from the geometrical center along the *x* axis direction.

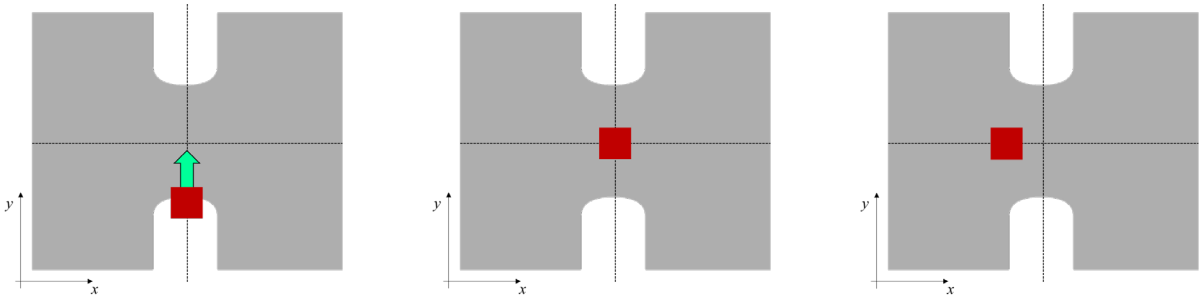


**Figure 2** The investigated heating strategies: a) LT, b) SPc, c) SPs

Laser heating was simulated implementing a temperature feedback loop by means of a DFLUX user subroutine: Table 2 lists the process parameters adopted for each of the mentioned strategies.

**Table 2** Process parameters adopted for the laser heating simulations

| Heating strategy | Temperature [°C] | Feed Rate [mm/s] | Dwell time [s] |
|---|---|---|---|
| LT | 550 | 3 | 3.3 |
| SPc | 550 | 0 | 5 |
| SPs | 550 | 0 | 5 |

At the end of each simulated condition, the nodal peak temperature was extracted, and the distribution of the variable *Ann* was estimated using the logistic function reported in Equation 2.

The switchover from the FE analysis of the laser heat treatment to the mechanical analysis of the specimen was carried out by extracting, as first step, the nodal maximum temperature values of the thermal model. Due to the small thickness of the specimen (2 mm), the structural analysis exploited the 2D plane stress condition as main assumption, using the Abaqus/Standard® CPS4R element type (4-node bilinear element with enhanced hourglass control); therefore, the nodal temperature values in the 3D space obtained from the thermal analysis has been interpolated onto the 2D mesh of the structural model by means of the Shepard algorithm, as input for the material model reported in Equation (3). All the constitutive equations were implemented in Abaqus/Standard® though an UMAT subroutine, adopting the common Euler Backward scheme for the numerical integration of the stress from the strain data. Other implicit or semi-implicit algorithms can be also used for the stress reconstruction, as, for instance, the one reported in [20] for large strain plasticity problems.

In this work, we also assumed an isotropic Von Mises plasticity behaviour, while the hardening behaviour of the AA5754 was described by using a modified version of the Voce's law according to a previous experimental investigation [17].

$$\sigma(\varepsilon_p) = Y(1+\varepsilon_p) - R\exp(-b\varepsilon_p). \quad (4)$$

All the material coefficients used in this numerical study, including the ones characterizing the logistic formulation in Equation 3, are listed in Table 3.

**Table 3** Coefficient of the constitutive equation

| Modified Swift hardening law | | | |
|---|---|---|---|
| Material state | $Y$ | $R$ | $b$ |
| As received (H32) | 232.74 | 98.32 | 20.08 |
| Fully annealed | 213.36 | 148.53 | 26.99 |
| Logistic hardening model | | | |
| $\beta$ | $c_\beta$ | $T^*$ | $\varepsilon_0$ |
| 0.01095 | 0.01423 | 301.35 | 0.005 |

## Results

Figure 3 reports the results from the thermal transient simulation. Contour maps of the nodal peak temperature (a, b and c) show that the irradiate portion of the specimen was properly heated at the specified temperature.

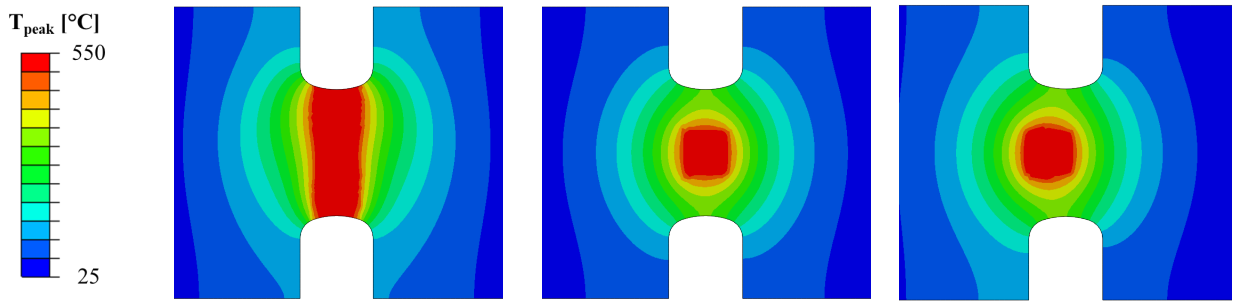


**Figure 3** Results from the thermal transient simulation: peak temperature and Ann variable distribution for the *LT* strategy (a), *SPc* strategy (b) and *SPs* strategy (c)

The effectiveness of the simulated heating was assessed by calculating the Ann variable along a 40 mm longitudinal path: results shown in Figure 4 demonstrate that the irradiated portion was effectively brought to the fully annealed condition (position *0* refers to the geometrical center of the notched specimen).

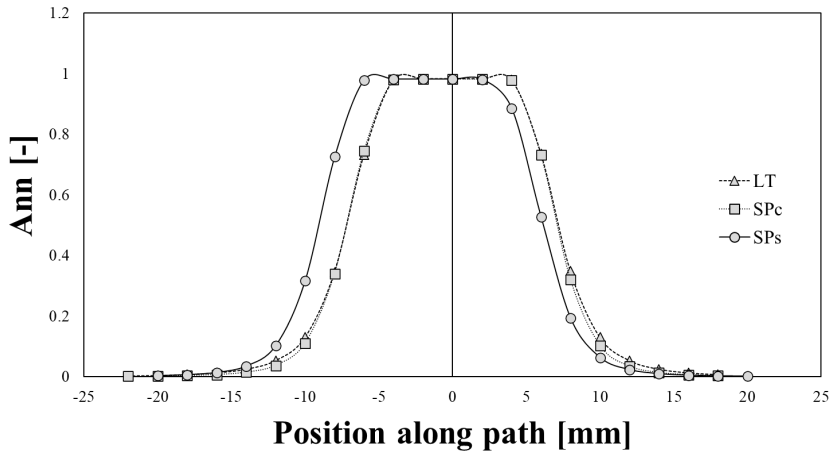


**Figure 4** Thermal simulations: distribution of the *Ann* variable along a longitudinal path

The evaluation of the heterogeneous strain (and stress) fields associated to the specimen deformation was performed on a confined region of the specimen around the two deep notches, as illustrated in Figure 5. The picture also shows the full-field map of the accumulated equivalent plastic strain $\bar{\varepsilon}_p$ imposing a horizontal displacement of 4.5 mm, before fracture occurs: for all the laser treatment strategies the strain localization occurs between the notches, exhibiting, however, a different maximum amounts of equivalent plastic strains according to the annealing pattern. It is worth noting that the higher values of $\bar{\varepsilon}_p$ reached by the specimen with the SPs treatment can be associated to the higher strength of the material in the gauge area between the two notches where the specimen has fewer material points at fully annealed state.

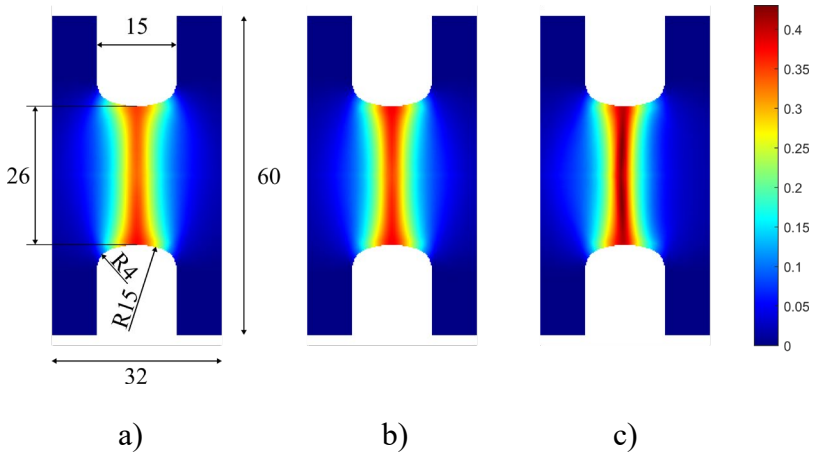


**Figure 5** Accumulated equivalent plastic strain on the central zone of the notched specimen with different tailored heat treatment: (a) LT strategy, (b) SPc strategy (c) SPs strategy. All the dimension indicated in (a) are in mm.

The heterogeneity of the mechanical states generated on the specimen was studied by using two main representations generally used to compare heterogenous mechanical tests [21]: the diagram of major and minor strains, reporting the principal strains of each material point, and the distribution of the stress states on the normalized stress plane. Although the latter representation is more common for displaying the material anisotropy according to the principal orientations of the material, it allows to better show the stress data on the yield surface.

Figure 6 depicts the mechanical states experienced by the specimen treated with the LT strategy, also displaying the corresponding maximum temperature as measure of the level of annealing produced by the local heating. The major vs. minor strains chart (Figure 6a) reveals that the fully annealed area (i.e. where the maximum temperature is close to 550°C) covers a wide area of strain states between the uniaxial tension and the plane strain tension states. Material points characterized by a lower treatment temperature (< 300°C) present a loading condition closer to the uniaxial tension,

mainly due to their position on the specimen surface, which is outside the two notches. The normalized stress plane chart in Figure 6b also suggests these conclusions, however, here it is also possible to observe the effect of the shear component, which allows to cover a large area of the yield surface. Nonetheless, the pure plane strain condition is not achieved, and only a restricted portion of the annealing spectrum gets closer to it.

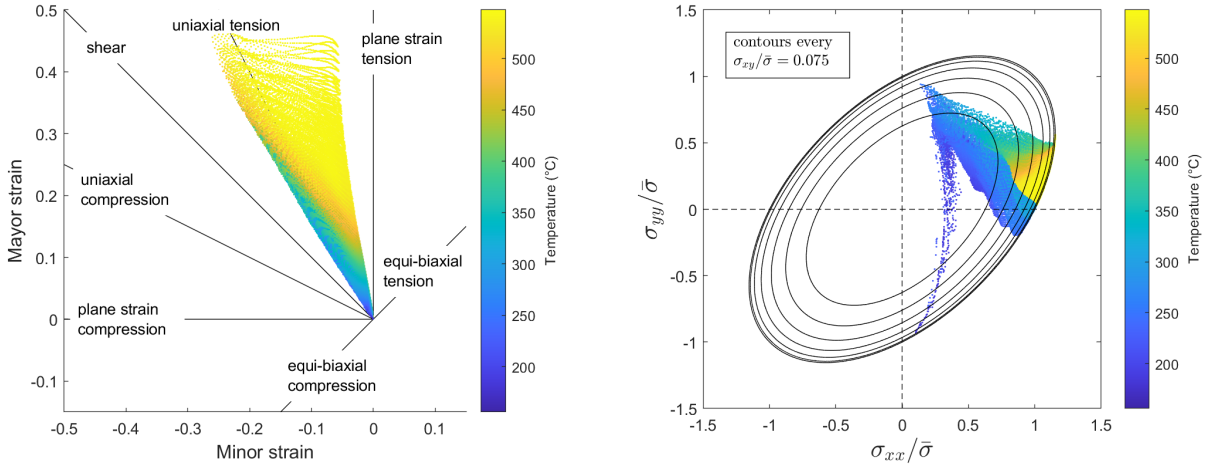


a) b)

**Figure 6** Distribution of major and minor strains (a) and stress states on the normalized stress plane for the notched specimen treated according to the LT strategy.

The concentrated laser spot (SPc) reduces the area between the two notches brought to the fully-annealed state. As consequence, material points with partial annealing covers a larger area between the uniaxial and the pure plane strain tension, with the fully-annealed ones confined in a small region close to the pure plane strain condition (Figure 7).

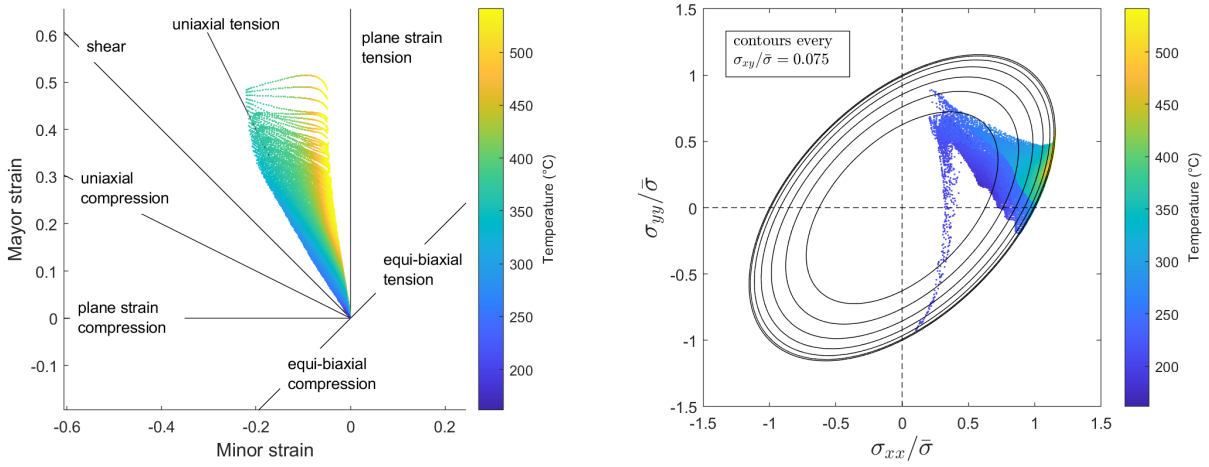


a) b)

**Figure 7** Distribution of major and minor strains (a) and stress states on the normalized stress plane for the notched specimen treated according to the SPc strategy.

Shifting the laser spot by 3.75 mm to the left allows to provide a wider range of annealing levels in the central part of the specimen between the two notches, where generally the plane strain condition is established during the deformation process (Figure 8). Interestingly, major vs. minor strain chart indicates that, during the last deformation stages, the minor strain remained almost constant, while the major strain increases up to fracture. In other words, the strain states for each material point treated with a temperature between 250°C and 550°C evolves along a vertical strain path, parallel to the pure plane strain tension condition.

The results show that the temperature distribution has a large impact in the stress state generated during the test, even if the geometry of the specimen does not change. In order to choose the best

solution for the thermo-mechanical material characterization, it is necessary to identify a metric or a numerical indicator to compare different temperature distribution, see for instance [21]. This is beyond the scope of this paper and will be addressed in future works.

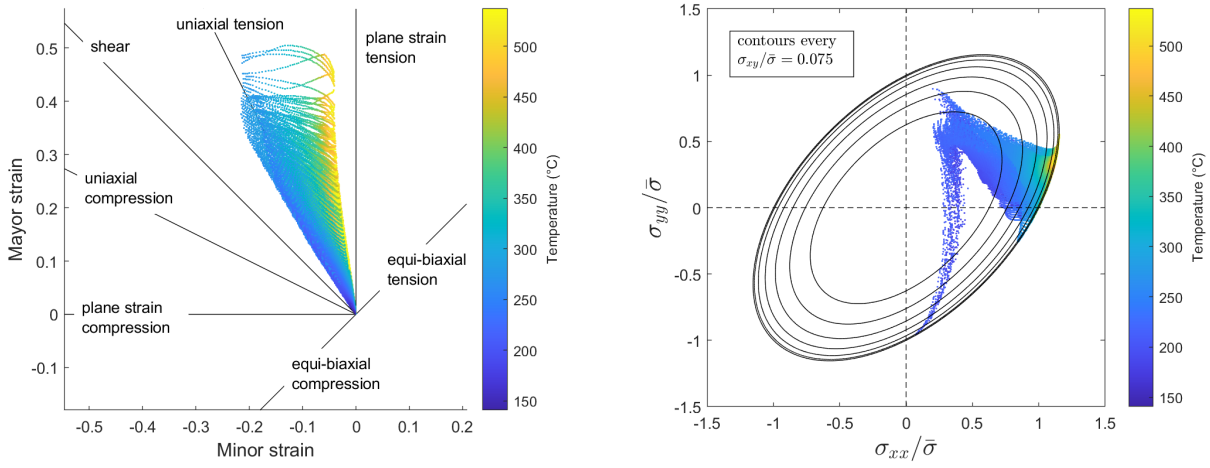


**Figure 8** Distribution of major and minor strains (a) and stress states on the normalized stress plane for the notched specimen treated according to the SPs strategy.

## Conclusions

In this work, a preliminary investigation on a quasi-homogeneous plane strain specimen for the simultaneous characterization of the annealing spectrum of metals is presented. The study exploited a numerical tool based on Finite Element simulations, which combines the simulation of a tailored heat treatment on sheet metals blanks with a structural analysis of the forming operations; in this way, it is possible to include all the details on the local variation of material properties produced by the annealing process by using a specific constitutive formulation expressing the hardening behaviour as function of the maximum treatment temperature.

The approach has been used to evaluate the heterogeneous strain (and stress) field created on a deep notched specimen, correlating the mechanical states with the annealing level produced according to three different treatment strategies. The heating pattern generated by a single laser spot allows to gather a wider distribution of the different annealing levels in proximity of the plane strain condition. As future developments, this first analysis opens to applications of the developed test in a more complex inverse identification framework. However, the specimen shape should be optimized considering important aspects such the statistical occurrence of the generated stress states, in order to verify the robustness and effectiveness of the proposed experimental procedure.

## References

[1] Taub, A., De Moor, E., Luo, A., Matlock, D. K., Speer, J. G., and Vaidya, U., 2019, "Materials for Automotive Lightweighting," Annu. Rev. Mater. Res., **49**(1), pp. 327–359.

[2] DIN EN 45545-2, 2016, "Railway Applications - Fire Protection on Railway Vehicles - Part 2: Requirements for Fire Behaviour of Materials and Components."

[3] Palumbo, G., and Piccininni, A., 2013, "Numerical-Experimental Investigations on the Manufacturing of an Aluminium Bipolar Plate for Proton Exchange Membrane Fuel Cells by Warm Hydroforming," Int. J. Adv. Manuf. Technol., **69**(1–4), pp. 731–742.

[4] Piccininni, A., Lo Franco, A., and Palumbo, G., 2022, "Warm Forming Process for an AA5754 Train Window Panel," J. Manuf. Sci. Eng., **144**(6), pp. 1–12.

[5] Geiger, M., Merklein, M., and Vogt, U., 2009, "Aluminum Tailored Heat Treated Blanks," Prod. Eng., **3**(4–5), pp. 401–410.

[6] Piccininni, A., and Palumbo, G., 2020, "Design and Optimization of the Local Laser Treatment to Improve the Formability of Age Hardenable Aluminium Alloys," Materials (Basel)., **13**(7).

[7] Rossi, M., Lattanzi, A., Piccininni, A., Guglielmi, P., and Palumbo, G., 2020, "Study of Tailor Heat Treated Blanks Using the Fourier-Series-Based VFM," Procedia Manuf., **47**, pp. 904–909.
[8] Sutton, M. A., Orteu, J. J., and Schreier, H. W., 2009, *Image Correlation for Shape, Motion and Deformation*, Springer.
[9] Pierron, F., and Grediac, M., 2012, *The Virtual Fields Method: Extracting Constitutive Mechanical Parameters from Full-Field Deformation Measurements*.
[10] Avril, S., Bonnet, M., Bretelle, A. S., Grédiac, M., Hild, F., Ienny, P., Latourte, F., Lemosse, D., Pagano, S., Pagnacco, E., and Pierron, F., 2008, "Overview of Identification Methods of Mechanical Parameters Based on Full-Field Measurements," Exp. Mech., **48**(4), pp. 381–402.
[11] Lecompte, D., Cooreman, S., Coppieters, S., Vantomme, J., Sol, H., and Debruyne, D., 2009, "Parameter Identification for Anisotropic Plasticity Model Using Digital Image Correlation," Eur. J. Comput. Mech., **18**(3–4), pp. 393–418.
[12] Grédiac, M., and Pierron, F., 2006, "Applying the Virtual Fields Method to the Identification of Elasto-Plastic Constitutive Parameters," Int. J. Plast., **22**(4), pp. 602–627.
[13] Rossi, M., Lattanzi, A., and Barlat, F., 2018, "A General Linear Method to Evaluate the Hardening Behaviour of Metals at Large Strain with Full-Field Measurements," Strain, **54**(3), p. e12265.
[14] Rossi, M., Pierron, F., and Štamborská, M., 2016, "Application of the Virtual Fields Method to Large Strain Anisotropic Plasticity," Int. J. Solids Struct., **97**–**98**, pp. 322–335.
[15] Lattanzi, A., Barlat, F., Pierron, F., Marek, A., and Rossi, M., 2020, "Inverse Identification Strategies for the Characterization of Transformation-Based Anisotropic Plasticity Models with the Non-Linear VFM," Int. J. Mech. Sci., **173**, p. 105422.
[16] Martins, J. M. P., Thuillier, S., and Andrade-Campos, A., 2021, "Calibration of a Modified Johnson-Cook Model Using the Virtual Fields Method and a Heterogeneous Thermo-Mechanical Tensile Test," Int. J. Mech. Sci., **202**–**203**, p. 106511.
[17] Lattanzi, A., Piccininni, A., Guglielmi, P., Rossi, M., and Palumbo, G., 2021, "A Fast Methodology for the Accurate Characterization and Simulation of Laser Heat Treated Blanks," Int. J. Mech. Sci., **192**(October 2020), p. 106134.
[18] Piccininni, A., Lattanzi, A., Rossi, M., and Palumbo, G., 2021, "Investigation of the Anisotropic Behaviour of Laser Heat Treated Aluminium Blank Blanks," **09**, pp. 1–9.
[19] Grytten, F., Holmedal, B., Hopperstad, O. S., and Børvik, T., 2008, "Evaluation of Identification Methods for YLD2004-18p," Int. J. Plast., **24**(12), pp. 2248–2277.
[20] Rossi, M., Lattanzi, A., Cortese, L., and Amodio, D., 2020, "An Approximated Computational Method for Fast Stress Reconstruction in Large Strain Plasticity," Int. J. Numer. Methods Eng., **121**(14), pp. 3048–3065.
[21] Oliveira, M.G., Thuillier, S., Andrade-Campos, A., 2021, "Evaluation of heterogeneous mechanical tests for model calibration of sheet metals." The Journal of Strain Analysis for Engineering Design: 03093247211027061.